Noncontact semiconductor wafer characterization with the terahertz Hall effect

D. M. Mittleman,[a] J. Cunningham, and M. C. Nuss[b]
Bell Laboratories, Lucent Technologies, Holmdel, New Jersey 07733

M. Geva
Lucent Technologies Microelectronics, Breinigsville, Pennsylvania 18031

(Received 19 December 1996; accepted for publication 26 May 1997)

We demonstrate noncontact measurements of the Hall mobility of doped semiconductor wafers with roughly 250 μm spatial resolution, using polarization rotation of focused beams of terahertz (THz) radiation in the presence of a static magnetic field. Quantitative and independent images of both carrier density and mobility of a doped semiconductor wafer have been obtained. © *1997 American Institute of Physics.* [S0003-6951(97)01427-7]

Doped semiconductors are frequently characterized by two material parameters, the carrier density N and the scattering time τ. These are important indicators of the sample properties and quality. They also determine many of the electrical and optical properties of the material. N and τ can be obtained via direct measurements of both the dc resistivity [proportional to $(N\tau)^{-1}$] and the Hall coefficient (proportional to N^1.) This method requires the sample under test to be contacted at four points and it averages over the portion of the sample in the region of the four probes, so that no information about spatial inhomogeneity in that region can be obtained. Spectroscopy with freely propagating electromagnetic radiation can address some of these issues.[1–7] In most of these measurements, the frequency dependence of the transmitted radiation was fit using an expression derived from the semiclassical Drude formalism to extract carrier density and scattering time. However, this fitting procedure generally cannot be accomplished rapidly enough to test for materials inhomogeneities in a practical imaging system. As a result, with few exceptions,[3,5,7] spatially resolved measurements of N and τ have not been performed.

In this letter, we demonstrate noncontact measurements of the Hall mobility of doped semiconductor wafers with roughly 250 μm spatial resolution. These measurements of the ''THz Hall effect'' are performed by measuring the polarization rotation of focused beams of THz radiation in the presence of a static magnetic field.[8,9] Our technique avoids time-consuming fitting procedures to extract N and τ, and thus, permits real-time extraction of these parameters. Therefore, quantitative real-time imaging of these semiconductor parameters can be performed. Separate images of both N and τ of a doped semiconductor wafer have been obtained.

Terahertz time-domain spectroscopy (THz-TDS) is a relatively new method for generating and detecting broadband subpicosecond pulses of far-infrared radiation.[10,11] This technique, based on the ultrafast gating of optoelectronic switches, has been demonstrated to be an extremely useful spectroscopic tool in the far infrared. More recently, the capabilities of THz-TDS have been extended to include the ability to form images.[12,13] Since the entire THz wave form (both amplitude and phase) is obtained at each pixel of the image, detailed physical or chemical information can be extracted at each point on the sample, with a spatial resolution limited only by the $\sim$250 μm spot size of the THz beam.

The THz Hall effect is conceptually identical to the familiar dc Hall effect. The THz field is focused onto the face of the doped semiconductor wafer under study, in the presence of a magnetic field pointing parallel to the beam propagation direction ($\hat{z}$). The applied THz field (polarized along $\hat{x}$) induces a current (also along $\hat{x}$), which in turn, induces a Hall current, oriented in the transverse direction (along $\hat{y}$). This Hall current radiates a THz field, which is coherent relative to the input THz beam, but which is polarized orthogonally to it. A measurement of the amplitude and phase of this radiated beam can be used to determine the full conductivity tensor of the sample. In practice, the incident field is polarized at 45° to the vertical axis, and both the vertical ($\hat{y}$) and horizontal ($\hat{x}$) fields are measured simultaneously, with two orthogonally oriented detectors.

The apparatus used for imaging with THz pulses has been described previously.[12] A schematic is shown in Fig. 1. For the Hall-effect measurements, the transmitter is oriented at 45° to the vertical, so the emitted radiation has approximately equal intensities along the vertical and horizontal axes. A free-standing wire grid polarizer is situated in front of the transmitter; this serves to clean up the polarization of the emitted light.[14] The sample is situated at the focus of the THz beam, in the bore of a permanent NdFeB magnet, which provides a field of roughly 1.3 T parallel to the THz beam propagation direction. A second free-standing grid acts as a polarizing beamsplitter[14] after the sample, to resolve the transmitted radiation into vertical and horizontal components. The signals from the two detectors are amplified in two current preamplifiers, and collected with a two-channel digital signal processor.

The samples consist of a 1 μm layer of doped GaAs, epitaxially grown on a semi-insulating GaAs substrate. These are mounted on a pair of translation stages, which move the sample relative to the (fixed) magnet and THz beam, in synchronization with the motion of the scanning delay line. In this fashion, images may be generated pixel by pixel.[12] The entire apparatus is covered in a plastic enclo-

[a]Current Address: Rice University, Electrical and Computer Engineering Dept., MS-366, 6100 Main St., Houston, TX 77005. Electronic mail: daniel@rice.edu
[b]Electronic mail: nuss@bell-labs.com

 0003-6951/97/71(1)/16/3/$10.00 © 1997 American Institute of Physics

Downloaded¬26¬Apr¬2001¬to¬128.42.4.78.¬Redistribution¬subject¬to¬AIP¬copyright¬or¬licence,¬see¬http://ojps.aip.org/aplo/aplcr.jsp

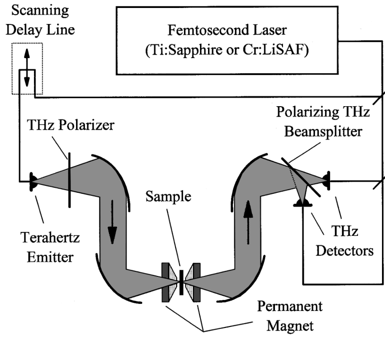

FIG. 1. Schematic of the experimental setup used for the measurements of the THz Hall effect. The apparatus is similar to that of Ref. 12, with the addition of a 1.3 T permanent magnet with optical access, a free-standing wire grid polarizing beamsplitter, and a second THz detector, oriented at 90° to the first. The THz emitter is oriented at 45°, to emit diagonally polarized radiation.

sure, which is purged with dry nitrogen to remove any water vapor from the THz beam path.

In the absence of a magnetic field (or in the absence of a sample), the optics (e.g., femtosecond laser power, beamsplitter alignment, etc.) can be adjusted so that the two measured fields are approximately equal. When the detectors are well aligned, only minor adjustments are necessary since the THz beam is well polarized at 45°. Then, when the magnetic field is applied to the sample, the degeneracy of these two fields is lifted. The difference between the two orthogonally polarized THz wave forms is a result of the THz Hall effect. This effect can be used to determine the carrier density and mobility, with the semiclassical Drude theory.

The Drude model fairly accurately describes the behavior of carriers in moderately doped semiconductors, even at THz frequencies.[6] In this formalism, the magnetoconductivity tensor has two independent values, the diagonal (σ_{xx}) and off-diagonal (σ_{xy}) elements. These are given by

$$\sigma_{xx}=\frac{\sigma_0\cdot(1-i\omega\tau)}{(1-i\omega\tau)^2+(\omega_c\tau)^2},\quad \sigma_{xy}=\frac{\sigma_0\cdot\omega_c\tau}{(1-i\omega\tau)^2+(\omega_c\tau)^2},\quad (1)$$

where ω_c is the cyclotron frequency, $\omega_c=eB/m^*c$. Because the doped layer is much thinner than one wavelength, the dc conductivity is proportional to the *sheet* carrier density, $\sigma_0=Ne^2\tau/m^*$. The transmitted fields can be determined by direct application of the Maxwell boundary conditions at the interface. These relate the incident, reflected, and transmitted waves to the induced surface current $J_s=\sigma(E_I+E_R)$.[16] By eliminating the two orthogonal components of the reflected wave, one can easily derive an expression for the field transmission coefficients in terms of the quantities in Eq. (1),

$$T_x=\frac{E_x^{\text{out}}(\omega)}{E_x^{\text{in}}(\omega)}=2\times\frac{1+n+Z_0\sigma_{xx}+Z_0\sigma_{xy}\cdot K(\omega)}{(1+n+Z_0\sigma_{xx})^2+(Z_0\sigma_{xy})^2}\times P(\omega),$$

$$T_y=\frac{E_y^{\text{out}}(\omega)}{E_y^{\text{in}}(\omega)}=2\times\frac{1+n+Z_0\sigma_{xx}-Z_0\sigma_{xy}\cdot K(\omega)^{-1}}{(1+n+Z_0\sigma_{xx})^2+(Z_0\sigma_{xy})^2}\times P(\omega).$$

Here, E^{out} (E^{in}) is the transmitted THz field measured with (without) the sample in place. Also, Z_0 is the impedance of free space, $Z_0\sim 377\Omega$, and n is the (frequency-dependent) refractive index of undoped GaAs.[16] Ideally, the two input fields $E_x^{\text{in}}(\omega)$ and $E_y^{\text{in}}(\omega)$ should be identical if the polarization of the input beam is precisely 45° and if the two detectors have identical responses and are precisely aligned. However, small differences inevitably persist. The factor $K(\omega)$ accounts for any such differences, $K(\omega)=E_y^{\text{in}}(\omega)/E_x^{\text{in}}(\omega)$. $P(\omega)$ describes the propagation of the radiation through the ~ 0.5 mm undoped substrate, as well as the transmission through the rear surface, using literature values for the optical properties of semi-insulating GaAs.[16] With this result, it is possible to relate the measured transmission coefficients T_x and T_y to the desired quantities N and μ in two equations, valid at any particular frequency within the bandwidth of the THz pulse. These equations can be analytically inverted and incorporated into the imaging routines, thus permitting real-time imaging of these two important material parameters.

It should be noted that this analysis neglects the effects of multiple reflections within the substrate. Such reflections are indeed observed, but they appear many picoseconds after the primary wave form. These secondary pulses can be safely removed from the data by time-domain windowing, before further processing.

In the absence of a magnetic field, the off-diagonal coupling vanishes, and it is no longer possible to extract both N and μ rapidly enough for imaging. Only the dc conductivity can be extracted, proportional to the product $N\mu$. Recent work by Livescu *et al.*[17] demonstrated that near-infrared photoluminescence imaging can also be used to measure this quantity. A comparison between these two methods has been performed, and the qualitative agreement is good. However, the photoluminescence technique is unable to extract quantitative information about the conductivity, or to distinguish between variations in doping density and carrier mobility.

In the presence of a magnetic field, the degeneracy between T_x and T_y is lifted (the Faraday effect), and now both carrier density and mobility can be extracted independently from these two measurements. In general, this requires a field large enough so that $\omega_c\tau$ becomes non-negligible. For a field of 1.3 T, $\omega_c\sim 2\pi\times 0.54$ THz for electrons in GaAs. For typical scattering times[6] of ~ 200 fs, $\omega_c\tau\sim 0.68$. Figure 2(a) shows the amplitude of the $\hat{x}$- and $\hat{y}$-polarized THz wave forms with no applied magnetic field, after having passed through a n-GaAs sample with a nominal doping density of 1.9×10^{17} cm^{-3}, as determined by growth conditions. Figures 2(b) and 2(c) show the same two spectra, except that the magnetic field has been applied parallel to the propagation direction in one case, and antiparallel in the other. The amplitudes of the THz waves are quite different in the presence of the field, and the sign of the difference changes with the sign of the field, a clear indication of the THz Hall effect.

Figure 3 shows two images, one for density [Fig. 3(a)] and one for mobility [Fig. 3(b)], of a portion of the wafer used in Fig. 2. In these images, the wave forms at each pixel were acquired by the digital signal processor, which performed a fast Fourier transform, extracted the electric fields at a preselected frequency (in this case, ~ 0.9 THz), and converted these field values into numerical estimates of N and μ using the formalism described above. The measured values are plotted as a greyscale. Inhomogeneities in both parameters are observed, with a length scale of ~ 1 mm.

In our initial experiment presented here, the measured values (both carrier density and mobility) are lower than the

Downloaded¬26¬Apr¬2001¬to¬128.42.4.78.¬Redistribution¬subject¬to¬AIP¬copyright¬or¬licence,¬see¬http://ojps.aip.org/aplo/aplcr.jsp

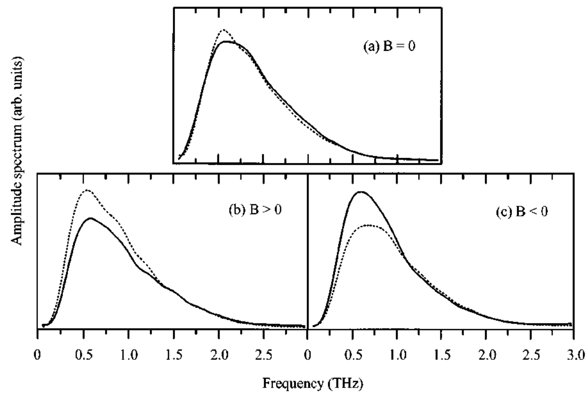

FIG. 2. THz wave forms transmitted through a n-doped sample. The nominal doping density for this sample was 1.9×10^{17} cm^{-3}. In each panel, the two curves correspond to the horizontal (solid) and vertical (dashed) components. In (a), no magnetic field is applied; in (b), a magnetic field parallel, and in (c), antiparallel to the THz beam propagation direction is applied.

parameters measured via electrical contact methods. We believe that this results from uncertainties in the value of B. The magnet used in these experiments produces a uniform field over only a rather small region. This difficulty can be overcome with the use of a larger magnet with a more homogeneous field distribution; without such a magnet, absolute determinations of the material parameters are difficult. In any event, the observed inhomogeneities in the wafer are quite reproducible from scan to scan, and almost certainly reflect true variations in the electrical properties of the semiconductor.

We would like to note that, for holes, $\omega_c \sim 2\pi \times 0.11$ THz in this magnetic field, and for typical valence-band scattering times of ~ 50 fs, $\omega_c \tau \sim 0.03$. Thus, it is somewhat more difficult to observe the THz Hall effect in p-doped samples. However, with the high signal-to-noise figures typical of THz-TDS, it should still be possible to detect effects on the level of a few percent. Small effects such as this have been difficult to observe here, in part because of the nonuniformity of the magnetic field mentioned above. Additionally, such observations have been hindered by the fact that, in order to obtain data with zero magnetic field, the entire magnet assembly has to be lifted out of the beam, which requires dismounting the sample. It would be far more elegant if the field could simply be switched externally. This would also afford the possibility of performing magnetic-field modulation experiments, in which extremely small effects should be detectable.

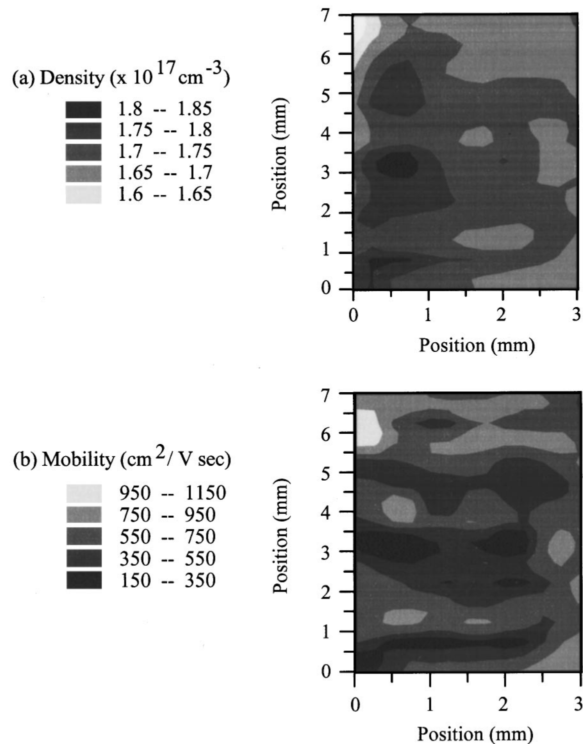

FIG. 3. THz images of a portion of a n-doped GaAs wafer. Variations in the doping density are shown in (a), while (b) shows inhomogeneities in the carrier mobility. The nominal doping density, as determined by growth conditions, is 1.9×10^{17} cm^{-3}.

The origin of the spatial variations observed in Fig. 3 is unclear. It is evidently related to parameters of the growth process. Secondary-ion-mass spectroscopy measurements on the same wafer also show carrier density variations that are of the order of 10%. Further experiments, involving *in situ* measurements, will be required to characterize this effect. In the transmission geometry employed here, this technique can be used to characterize samples with sheet densities in the range from 5×10^{12} cm^{-2} up to $\sim 10^{15}$ cm^{-2}.

In summary, subpicosecond pulses of freely propagating THz radiation have been used to drive a Hall current in moderately doped semiconductor samples immersed in a dc magnetic field. This Hall current oscillates at THz frequencies, and thus radiates another THz field, polarized orthogonally to the driving field. This effect has been used to extract the full complex conductivity of the semiconductor, just as in the traditional Hall effect, but without making any contacts to the sample. This high-frequency Hall effect has been combined with the THz imaging technology to provide a method of characterizing spatial inhomogeneities in both doping density and carrier mobility. Recent work, which has extended the imaging capability to a reflection geometry,[13] should permit similar THz Hall-effect experiments on opaque samples, such as highly doped semiconductors or metals.

[1] J. Kudman, J. Appl. Phys. **34**, 1826 (1963).
[2] J. D. Holm and K. S. Champlin, J. Appl. Phys. **39**, 275 (1968).
[3] J. F. Black, E. Lanning, and S. Perkowitz, Infrared Phys. **10**, 125 (1970).
[4] B. L. Bean and S. Perkowitz, J. Opt. Soc. Am. **67**, 911 (1977).
[5] T. Ohba and S. Ikawa, J. Appl. Phys. **64**, 4141 (1988).
[6] N. Katzenellenbogen and D. Grischkowsky, Appl. Phys. Lett. **61**, 840 (1992).
[7] M. Golosovsky and D. Davidov, Appl. Phys. Lett. **68**, 1579 (1996).
[8] R. G. Chambers and B. K. Jones, Proc. R. Soc. London, Ser. A **270**, 417 (1962).
[9] S. Spielman, B. Parks, J. Orenstein, D. T. Nemeth, F. Ludwig, J. Clarke, P. Merchant, and D. J. Lew, Phys. Rev. Lett. **73**, 1537 (1994).
[10] P. R. Smith, D. H. Auston, and M. C. Nuss, IEEE J. Quantum Electron. **24**, 255 (1988).
[11] C. Fattinger and D. Grischkowsky, Appl. Phys. Lett. **54**, 490 (1989).
[12] B. B. Hu and M. C. Nuss, Opt. Lett. **20**, 1716 (1995).
[13] D. M. Mittleman, R. H. Jacobsen, and M. C. Nuss, IEEE J. Sel. Top. Quantum Electron. **2**, 679 (1996).
[14] W. G. Chambers, C. L. Mok, and T. J. Parker, J. Phys. A **13**, 1433 (1980).
[15] M. C. Nuss and J. Orenstein, in *Millimeter-Wave Spectroscopy of Solids*, edited by G. Gruener (Springer-Verlag, Heidelberg, 1997).
[16] D. Grischkowsky, S. Keiding, M. van Exter, and C. Fattinger, J. Opt. Soc. Am. B **7**, 2006 (1990).
[17] G. Livescu, M. Angell, J. Filipe, and W. H. Knox, J. Electron. Mater. **19**, 937 (1990).

Downloaded¬26¬Apr¬2001¬to¬128.42.4.78.¬Redistribution¬subject¬to¬AIP¬copyright¬or¬licence,¬see¬http://ojps.aip.org/aplo/aplcr.jsp